International Conference on Space Optics—ICSO 2018

Chania, Greece

9–12 October 2018

Edited by Zoran Sodnik, Nikos Karafolas, and Bruno Cugny

The European CO2 Monitoring Mission: observing anthropogenic greenhouse gas emissions from space

Bernd Sierk

Jean-Loup Bézy

Armin Löscher

Yasjka Meijer

The European CO_2 Monitoring Mission: Observing anthropogenic greenhouse gas emissions from space

Bernd Sierk[a], Jean-Loup Bézy[a], Armin Löscher[a], Yasjka Meijer[b]
[a]ESA-ESTEC [b]; Rhea for ESA-ESTEC

ABSTRACT

Responding to plans of the European Commission for extending the observation capabilities of the Copernicus programme, the European Space Agency (ESA) has initiated Phase A industrial (technical feasibility) studies for several new space-borne Earth Observation missions. High priority is given to a constellation of LEO satellites in Sun-synchronous orbit with the purpose of observing anthropogenic carbon dioxide (CO_2) emissions [European Commission, 2017]. The observing system shall acquire images of CO_2 concentration in terms of dry air column-averaged mole fractions (XCO_2), providing complete global land coverage at high spatial resolution (4 km^2) within five days. The demanding requirements call for a payload comprising a combination of multiple instruments, which perform simultaneous measurements. The XCO2 is inferred from reflectance measurements in the Near-Infrared (NIR) and Short-Wave Infrared spectral regions (SWIR). This requires at least three spatially co-registered push-broom imaging spectrometers, measuring spectral radiance and solar irradiance in the NIR (747-773 nm), SWIR-1 (1595-1675 nm) and SWIR-2 (1990-2095 nm) at moderate spectral resolving power (R~5000-7000). In addition, the observations for CO_2 concentration will be complemented by Differential Optical Absorption Spectroscopy (DOAS) measurements of nitrogen dioxide (NO_2) over the same area. The NO_2 measurements in the visible region (400-500 nm) are expected to serve as a tracer for plumes of high CO_2 concentration resulting from high temperature combustion, which will facilitate plume identification and mapping. The third component of the payload is a multiple-angle polarimeter (MAP), performing high-precision measurements of aerosol (and cloud) properties. Its measurements of polarized radiance under various observation angles are expected to reduce XCO_2 bias error and significantly increase the yield of useful retrievals from the NIR and SWIR spectra. The complex observation architecture, involving multiple instruments and platforms, call for optimized observational requirements, driven by the primary goal of detecting and quantifying point-sources of greenhouse gas emissions. In particular, high single-sounding precision is essential for identifying plumes of elevated CO_2 concentration from instantaneous image acquisitions without regional and temporal averaging. This translates into stringent requirements for Signal-to-noise ratio (SNR), as well as spatial co-registration and spectral stability, which drive the instrument design. The presentation will introduce the different elements of the candidate Copernicus mission, in view of the ambitious mission goals. The payload components and observation requirements are addressed with special emphasis on the derivation of the SNR and spectral resolution requirements, which determine the instrument sizing.

Keywords: Imaging spectrometer, Copernicus programme, anthropogenic CO_2, greenhouse gas observation

1. INTRODUCTION

In 2015 world leaders gathered in Paris to agree on how to combat climate change, as it is now well established that anthropogenic emissions of greenhouse gases need to be significantly reduced [1]. International treaties and agreements, aiming at reducing emission from fossil fuel combustion have been singed by many nations. While the targeted emission reductions are based on voluntary Nationally Determined Contributions (NDCs), there is a future demand of actionable information on the effectiveness of implemented measures and regulations. In this context, the European Commission has formulated a system architecture with Monitoring and Verification Support capacity[2]. An earlier report identified the need of a multi-component observation system for quantification and monitoring of anthropogenic greenhouse gas emissions requires, involving in-situ and remote sensing observations on various spatial domains [3]. One of the main pillars, besides on-ground measurements relies on space-borne observations of the concentrations of the most important anthropogenic greenhouse gases, carbon dioxide (CO_2) and methane (CH_4). The high-level observation requirements call for a multi-satellite constellation with imaging capability at high spatial resolution, global coverage and frequent re-visit.

Measurements of column averaged dry air mole fractions of carbon dioxide (XCO_2) and methane (XCH_4) have been pioneered by the SCIAMACHY instrument on-board ESA's Envisat satellite[4]. After the launch failure of NASA's Orbiting Carbon Observatory (OCO,[5]) in 2009, JAXA's GOSAT became the first dedicated mission to target CO_2 and CH_4 measurements from space[6]. GOSAT performs measurements of top-of-atmosphere (TOA) spectral radiance by means of a Fourier Transform Infrared Spectrometer (FTIR), with large distances between single soundings (X km). In August 2014 NASA successfully launched OCO-2 [7] and has since been providing continuous soundings of XCO_2 at high spatial resolution (~ 3 km^2). The OCO-2 instrument is a three-band grating spectrometer operated in push-broom mode. Despite of its narrow swath width ($\sim$20 km) and incomplete global coverage, OCO-2 has demonstrated the capability of imaging point sources, such as power plants [8]. In December 2016, the Chinese TanSat mission was launched[9], which has similar spatial resolution and coverage, and first results have recently been published[10]. Currently, there are several future missions under preparation, most notably MicroCarb (led by CNES) [[11]] and the geostationary GeoCarb (University of Oklahoma) [12], which also feature high spatial resolution modes for point-source observation. Based on the results of previous and on-going missions and instrument studies, there is now considerable heritage of space-borne greenhouse gas observations to design a system dedicated to anthropogenic CO_2 monitoring.

In this context, the European Space Agency (ESA) has initiated technical feasibility (Phase-A) studies with two industrial consortia led by Airbus Defense and Space and OHB, respectively. The studies are part of a series of Phase-A studies aiming at extending the capabilities of the Copernicus programme. In this frame, a potential future CO_2 monitoring mission, in the following referred to as CO2M, could be a candidate for a future Sentinel mission. In preparation and support of the industrial activities, two scientific studies with the objectives of identifying the observation requirements for a constellation of satellites equipped with a suite of instruments optimized for anthropogenic CO_2 monitoring. The SMARTCARB study performed by a consortium led by Swiss Federal Laboratories for Materials Science and Technology (EMPA), is addressing potential synergies of measurements for observing and quantifying CO_2 point sources such as large cities and power plants. Also, the impact of different satellite specifications (e.g. overpass time and spatial coverage) are investigated. The AEROCARB study, performed by a consortium led by the Space Research Organization of the Netherlands (SRON), investigates the use of auxiliary measurements to better constrain the atmospheric aerosol and cirrus cloud distribution over the sampled areas, which was identified to be a significant limitation for accurate XCO_2 retrieval.

This paper presents the driving mission and observation requirements identified in these and earlier studies, as well as the implications for the instrument architecture. It also addresses the translation from Level-2 (concentrating on XCO_2), to calibrated radiance measurements (Level-1b), with special emphasis on the driving signal-to-noise ratio (SNR) requirement.

2. MISSION OBJECTIVES AND REQUIREMENTS

The principle science goals of past and current space-borne missions for observation of XCO_2 and XCH_4 are related to the global carbon cycle and the identification and quantification of natural sources and sinks of greenhouse gases. Anthropogenic fluxes of CO_2 are typically an order of magnitude weaker than biogenic fluxes and therefore more difficult to quantify and separate from the latter. Emission from fossil fuel combustion can only be detected in the vicinity of strong point sources. Significantly elevated values for XCO_2 in excess of a few percent of the background value ($\sim$390 ppm) can be detected within down-wind plumes of coal-fired power plants, and potentially large cities. Since the well-mixed gas CO_2 is quickly diluted after emission, the expected signal of enhanced XCO_2 depends on the size of the observed spatial samples (spatial resolution) and the wind speed.

Space-borne quantification and monitoring of anthropogenic greenhouse gas emission sources has not yet been established as an operational observing method. However, requirements for a space-borne component of an operational monitoring system have been identified in an expert study funded by the European Commission [3]. According to the report, monitoring of anthropogenic carbon emissions require a satellite constellation, observing XCO_2 at high precision (< 0.7ppm) and low systematic bias (< 0.5 ppm) with global coverage every 2-3 days. ESA has initiated scientific support studies to further consolidate observational requirements with particular emphasis on the precision (repeatability) and accuracy (systematic bias) of the XCO_2 observations. The precision is mainly determined by the signal-to-noise ratio (SNR) of the measured TOA spectral radiance, and pseudo-noise from spatial co-registration and radiometric scene non-uniformity. Systematic biases may be introduced by instrumental errors like straylight, polarization sensitivity and detection non-linearity, as well as by geophysical effects, like the uncertainties in the aerosol distribution above the scene. The instrumental and geophysical error sources affecting the retrieval of XCO_2 from space-borne measurements

of spectral radiance call for an observing system with multiple sets of combined observations. In the following we summarize the mission requirements for these different sets of observations.

3. PAYLOAD ELEMENTS AND OBSERVATION MODES

3.1 Payload components

Recognizing the challenging task of operational, quantitative monitoring of greenhouse gas sources and sinks and distinguishing anthropogenic from biogenic emissions, the CO2M mission advisory group recommended a combination of multiple payloads. The principal instrument will measure Top-Of-Atmosphere (TOA) spectral radiance in three continuous spectral intervals: The Near-Infrared (NIR) encompassing the oxygen (O_2) A-band, and two Short-Wave Infrared (SWIR) bands covering three CO_2 and one CH_4 absorption band. The band definition is further detailed in Section 5.1. The CO_2 instrument will be based on a push-broom imaging spectrometer concept for simultaneous and co-located observation in all spectral bands. The measurement principle is described in [13] and recalled in Figure 1.
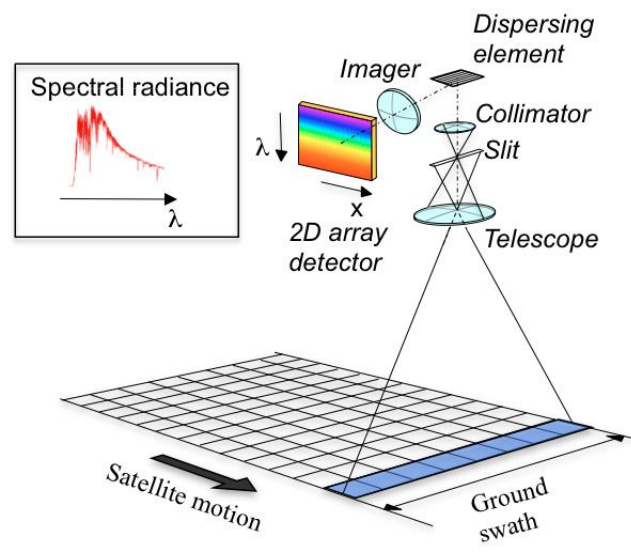
4.

Figure 1: Principle of a push-broom imaging spectrometer. The entrance slit of the spectrometer is imaged onto the Earth surface, defining the swath width in across-track direction. The instrument spectrally disperses the slit image in along-track direction, which is sampled by the spacecraft motion during integration time. The products for each spatial sample are inferred from radiance spectra imaged onto the 2D array detector.

In support of the XCO_2 retrieval, the need of additional measurements of the aerosol and cirrus cloud distribution above the sampled area was identified. The general observation principle consists in the measurement of polarized radiance under various viewing directions. This component of the instrument suite is referred to as a Multiple-Angle-Polarimeter (MAP). The complementary MAP observations can be performed by different types of instruments, which are closer described in Section 5.6.

In order to improve the capability for emission plume identification and mapping, an additional imaging spectrometer operating in the visible (VIS) spectral region is required. The objective is to measure column densities of tropospheric nitrogen dioxide (NO_2). Such observations can be used as a tracer for CO_2 from anthropogenic high-temperature combustion processes, as shown in Figure 2 and further explained in Section 5.5. Extensive heritage exists for space-borne NO_2 mapping from previous and on-going atmospheric chemistry missions, like the recently launched Sentinel-5P [15]. However, the requirements for the CO2M mission call for an unprecedented spatial resolution of such observations (2 km x 2km).

Finally, the expert team identified the need for cloud-flagging and characterization for all acquired spatial samples. Strong cloud cover can already be detected from observations of the three previously described payload components.

However, scattering within small, sub-sample sized clouds as well as subvisible cirrus clouds lead to light-path modulation, which is difficult to distinguish from enhanced CO_2 concentration. The strong sensitivity of the XCO_2 retrieval to cloud contamination calls for a cloud-imager capable of detecting small tropospheric clouds and cirrus cover at a spatial resolution exceeding those of the other payload components. The resulting requirements are summarized in Section.
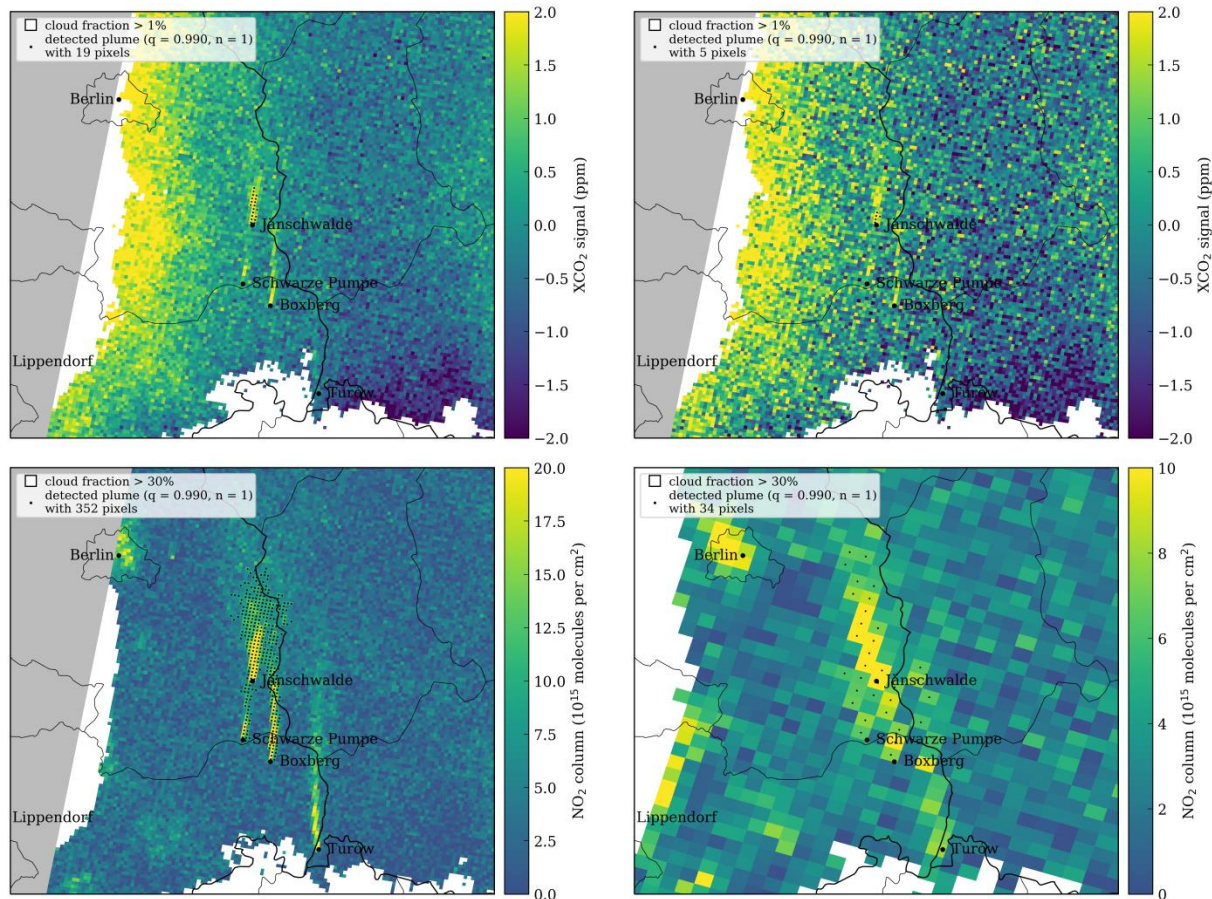

Figure 2: Example of plume detection for several power plants in East Germany. The simulated images depict XCO_2 (upper row) as well as NO_2 columns(lower row) at CO2M spatial resolution (4 km^2). The upper left image assumes a random error of of 0.5ppm and the upper right plot the correposnding image for 1.0 ppm precision. The lower left image shows the strong correlation of the NO_2 plumes with those of CO_2 emission. The lower right image depicts the same NO_2 scene coarser spatial resolution comparable to Sentinel-5 (7km x 7 km), demonstrating the loss of the capability to distinguish the individual emission sources. Courtesy EMPA.

4.1 Observation modes and coverage

All instruments will perform simultaneous and spatially co-located observations with different spatial co-registration requirements. Various observation modes under different geometric conditions are foreseen. The most important one is the nadir mode, in which the field-of-views of all instruments are directed towards the sub-satellite point (apart from the off-nadir viewing angles of the MAP instrument). The second principal Earth observation mode enables observations in the Sun-glint geometry. In this mode, the CO_2 instrument will be directed pointed the area of specular reflection of sunlight, which can be achieved either via a scan mirror or by a platform maneuver. Due to the very low reflectance of water bodies in the SWIR bands, measurements over oceans are only possible in Sun-glint mode. In addition, Sun-glint observations over land may be useful, especially over lakes and snow-covered or poorly illuminated regions. The two Earth observation geometries are complemented by calibration modes, which enable in-flight radiometric characterization using direct observation of the Sun (e.g. via solar diffuser), and geometric calibration using the Moon.

Targeting an operational global observing system, stringent observation requirements for coverage and re-visit have been established. The expert team of the mission advisory group recommended complete geometrical land coverage within 2-3 days pole-ward of 40° latitude, and within 5 days at the equator. Since the field-of view, and consequently the swath width of the above instruments is limited by technical (detector size) constraints as well as retrieval limitations (Solar Zenith Angle (SZA)), the coverage achievable with a single spacecraft call for a multi-platform constellation.

5. SYSTEM REQUIREMENTS

5.1   Spectral requirements for XCO₂ observations

Accurate determination of XCO_2 from simultaneous three-band retrieval has been demonstrated with measurements from OCO-2 and GOSAT [e.g. [16]]. Observations of the oxygen (O_2) A-band in the NIR spectral region are required to determine the effective light propagation in the radiative transfer model used in the retrieval algorithm, making use of the known concentration of the well-mixed oxygen. In the SWIR spectral region, rotation-vibrational molecular transitions of the CO_2 molecule give rise to absorption lines concentrated in spectral intervals around 1.6 µm, 2.0 µm and 2.04 µm (see Figure 3). The heritage missions GOSAT and OCO-2 sample these regions in relatively narrow spectral intervals at a spectral resolution sufficient to resolve individual absorption lines (R>20.000). While high spectral resolution is advantageous for reducing systematic biases (e.g. from unknown aerosol distribution), it handicaps high signal-to-noise (SNR) observation because of the lower spectral sampling interval per pixel. For contiguous mapping of CO2 concentration around point sources and their local vicinity, large SNR of the measured radiance, maximizing single-sounding precision of XCO_2, has higher priority than for climate missions primarily targeting the stronger biogenic fluxes. Low measurement noise is especially important for instantaneous imaging of emission plumes, which depend on actual wind and aerosol conditions at the time of the over-flight.

Spectral Band ID	Spectral Range [nm]	Spectral Resolution Δλ [nm]	Spectral Sampling Ratio
NIR	747 – 773	0.12	3.0
SWIR-1	1590 – 1675	0.30	3.0
SWIR-2	1990-2095	0.35	3.0

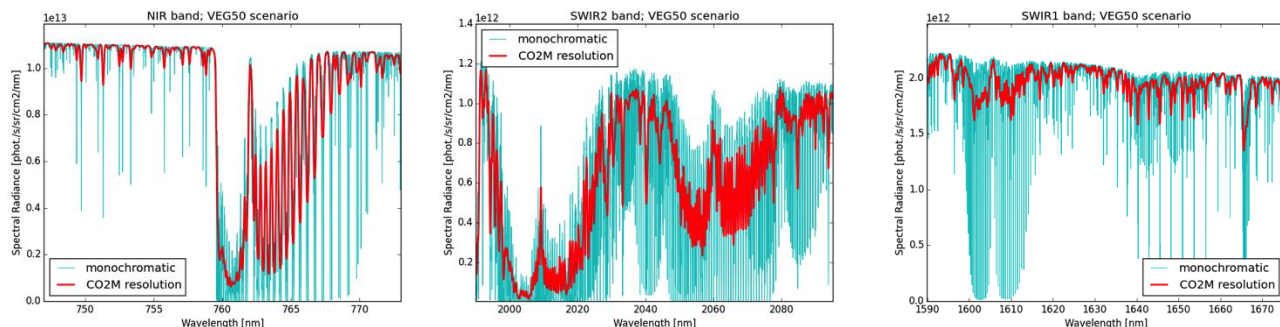Table1: Spectral band definition for the CO2M mission.

Figure 3: Top-of-atmosphere radiance spectra of the three bands used for XCO2 retrieval, both incident monochromatic and at spectral resolution of the CO2-instrument.

In this context the requirements for spectral bandwidth, resolution and SNR have been derived in order to optimize the CO2M observations with respect to the primary mission goal of point source monitoring. A large number of retrieval simulations have been performed at different resolutions, bandwidths and SNR. The results indicate optimum imaging performance for medium spectral resolution around 0.3 nm (R~5000), while the bandwidth needs to be sufficiently wide to completely cover the absorption bands and the continuum at their spectral boundaries. The analysis confirmed that the loss of information by reduced spectral resolving power is compensated by the larger bandwidth (more CO_2 lines

measured) and correspondingly higher SNR (see below). The spectral band requirements are summarized in Table 1, and the spectral radiance at instrument resolution for the geophysical reference scenario is depicted in Fig. 3.

The retrieval simulations performed for optimizing spectral resolution and bandwidth were also used to derive the SNR requirements, which determine the sizing of the instrument. As mentioned above, the lower spectral resolving power targeted for CO2M in comparison with heritage missions needs to be compensated by correspondingly higher SNR. The noise level of the Level-1b radiance measurements directly affects the precision of the Level-2 product (XCO$_2$ in ppm), which in turn limits the detectability of point sources the accuracy of CO$_2$ flux inversions. Therefore the derivation of the SNR requirement started from using flux inversion simulations for a range of assumed XCO$_2$ precisions. Figure 2 depicts simulated images of XCO$_2$ and NO$_2$ over an area in East Germany, where several coal-fired power plants are located. The imager in the upper row of the figure represent the same geophysical scenario measured with different precision (noise) levels in XCO$_2$ at the spatial resolution of the CO2M instrument (4 km^2).

The plots give an impression of the spatial extent and variability of typical emission plumes, as well as on the impact of retrieval noise on the capability to distinguish the plume from the background concentration.

5.2 Signal-to-noise requirements for XCO$_2$ observations

For the purpose of mission requirement derivation, a geophysical scenario reference scenario was defined, corresponding to an observation geometry with a moderately low solar zenith angle of 50° and relatively low typical for albedo vegetation. In the following this geophysical reference scenario is referred to as VEG50. With flux inversion simulations over this scene at the given spatial resolution of 4 km^2 it was established, that an XCO$_2$ single-sounding retrieval precision of 0.7 ppm is required for sufficiently accurate quantification of point source emissions. As this represents the maximum tolerable random error of the retrieval, a goal precision of 0.5 ppm was established, providing for margin for other error contributors, like pseudo-noise from spatial co-registration or scene non-uniformity.

These Level-2 precision requirements were linked to the radiometrically calibrated (Level-1b) measurements via a large number of retrieval simulations with generalized instrument parameters. The basic assumption is that the signal-to-noise ratio of the instrument can be expressed by a simple combination of two noise components, and for any measured spectral radiance L is expressed by:

$$ SNR = \frac{A \times L}{\sqrt{A \times L + B}} \ , \quad (1) $$

The parameter A represents the signal-dependent shot-noise, and depends on various instrument parameters:

$$ A = \hbar \cdot T \cdot D\lambda \cdot QE \cdot t_{int} \cdot N_{bin,X} , \quad (2) $$

where η is the etendue of the instrument, T the total transmission; $\Delta\lambda$ the spectral sampling interval, QE the quantum efficiency of the detector. $N_{bin,X}$ represents the number of detector pixels co-added to form the across-track field of view of a spatial sampling, and t$_{int}$ the exposure time over which it is acquired (defining the along-track sampling distance).

The second parameter of Eq. (1) encompasses the signal-independent instrumental noise sources, e.g. from kTc noise of the read-out circuit or digitization noise. In our analysis it is modeled as

$$ B = N_{bin,X} \times \sqrt{\left(I_{dark} + I_{Tb}\right) \times t_{int} + \left(N_{AD}^2 + N_{RO}^2 + N_{VC}^2\right) \times N_{temp}} \ , \quad (3) $$

where $I_{dark:}$ is the dark current, $I_{Tb:}$ shot noise from background thermal emission, N_{RO} the detector read-out noise, N_{AD} thedigitization noise, and N_{VC} the video chain noise. In the case of several read-outs per integration time, N$_{temp}$ represents the temporal sampling factor.

While equations (1) – (3) are generally valid for simulating the SNR of any push-broom imaging spectrometer, the number of parameters indicates a large parameter space, which renders the task of deriving a generalized SNR requirement a complex task. However, by assuming a realistic range of values for parameters *A* and *B*, computed from Eq. (2) – (3), and using Eq. (1) to simulate the noise of the reference spectra (see Figure 3), we can derive the dependencies of XCO$_2$ retrieval precision from signal-dependent and –independent noise components. As will be shown

below, from these we can find pivotal tuples of spectral radiances and associated SNR values, which correspond to the required Level-2 precision.
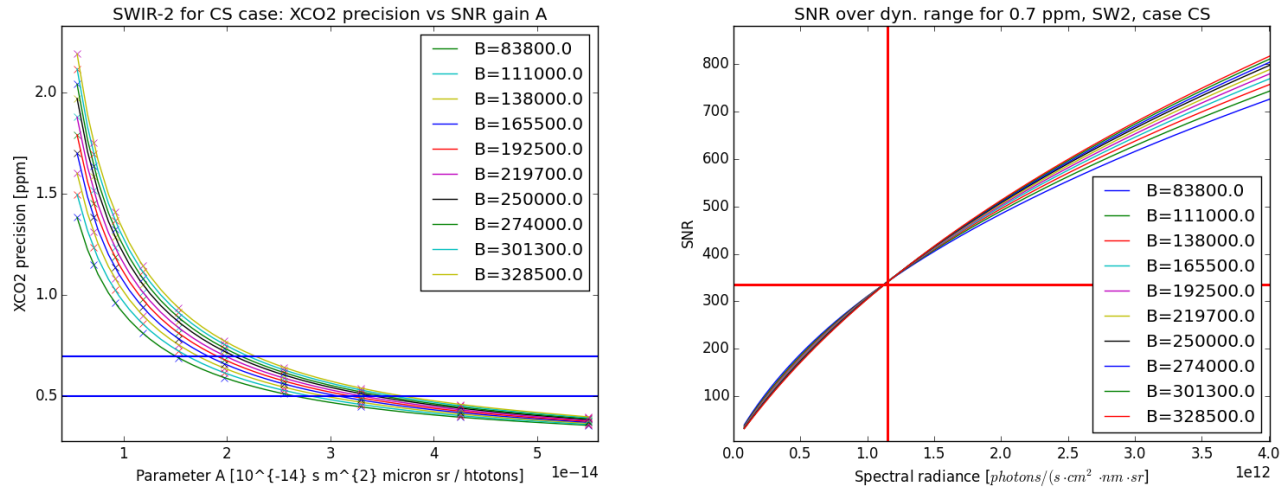

Figure 4: a) left: Simulated XCO2 precision as a function parameter A, representing the signal-dependent shot noise component, for various B-values (signal-independent noise component). The blue horizontal lines represent the threshold (0.7ppm) and goal (0.5ppm) precision requirements. The intersection of the lines with the curves define combinations (A,B), which comply with the Level-2 requirement. Right panel: SNR performance as a function of incident spectral radiance for the identified (A,B) combinations from the left panel. The curves describe the SNR dependence of compliant instruments with different signal-independent noise (e.g. from different read-out noise). The curves intersect in one point (indicated by the red lines), which defines the required SNR at a reference radiance Lref.

Figure 4a (left plot) shows a plot of simulated XCO_2 precision as a function of parameter A for a family of curves corresponding to different signal-independent noise levels. Each single curve represents an assumed instrument with a combination of dark- and readout-noise yielding its value of B, and shows the dependence of the resulting XCO_2 precision from the signal-dependent parameter A. For a given instrument setup with fixed detection parameters (e.g. read-out and video-chain noise, etc.), the curves in Fig. 2a identify the required value of A for any desired Level-2 precision. If all other instrument parameters in Eq. (2) are fixed (transmission, spectral resolution, quantum efficiency, integration time, and over-sampling), the A value can be translated into the pupil size needed to reach the required measurement precision. The horizontal lines in Figure 4a indicate the targeted threshold and goal precisions (0.7 ppm and 0.5 ppm, respectively). The intersection of these lines with the performance curves yield combinations of A and B, for which the required precision is reached. Therefore, each pair (A,B), defined by the intersection of the threshold (resp. goal) line, corresponds to an instrument yielding exactly 0.7 ppm (resp. 0.5 ppm) precision in XCO_2.

The compliant instruments identified this way are characterized by their SNR dependence from incident radiance according to Eq. (1), which is plotted in Figure 4b (right plot). Each such instrument described by a selected (A,B) combination yields the exact same Level-2 precision for the reference scenario (VEG50). However, those corresponding to low values of B exhibit slightly higher SNR at lower radiances, but lower SNR at brighter radiances, than the SNR-curves for large values of B. This is expected, as in the low radiance regime the signal-independent noise component is more important, while at high radiances the SNR is dominated by shot noise. Instruments with relatively high read-out noise (large B) require a greater étendue (e.g. large entrance pupil size) to compensate, and therefore perform better at the bright end of the dynamic range. Because of the described behavior of the SNR-curves in Figure 4b they intersect with each other at a point, where the signal-independent (read-out noise) dominated regime passes into the shot-noise domain. At the radiance level L_{ref} defined by this point, all instruments setups selected by the intersection of the threshold line in Figure 4a measure with the same SNR performance (SNR_{ref}). This pivotal point (L_{ref}, SNR_{ref}) is used to define a simple SNR requirement, as any instrument measuring with SNR_{ref} at L_{ref} will yield a precision equal to the required 0.7 ppm (resp. 0.5 ppm).

The derivation of the SNR requirement described above is performed simultaneously for the SWIR-1 (1595nm-1675nm) and SWIR-2 (1990nm - 2095nm) bands. It turns out that in both SWIR bands the value for SNR_{ref} is the same and fixed by the required XCO2 precision, while the value for L_{ref} depends on the required spectral resolution. The values found for the CO2M mission are listed in Table X. It is important to note that the derivation of the SNR requirement described above does not depend on any assumption on the instrument, like a particular detector type (read-out noise), pupil size, or binning factor. Since the two free parameters A and B encompass all instrumental effects included in the simulation and Eq. (2) and (3), the requirements in Table 2 ensure the required XCO2 precision for a broad range of possible instruments with different detector performances and entrance pupil size.

Spectral Band ID	L_{ref} [ph./s/cm2/nm/sr]	SNR$_{ref}$ (Threshold, 0.7ppm)	SNR$_{ref}$ (Goal, 0.5ppm)
NIR	$4.20 \cdot 10^{12}$	260	330
SWIR-1	$2.15 \cdot 10^{12}$	345	500
SWIR-2	$1.85 \cdot 10^{12}$	345	500

Table 2: SNR requirements for the CO2 instrument of the CO2M mission

5.3 Spatial co-registration for XCO2 observations

Apart from measurement noise, another source of random error, limiting the capability to quantitatively characterize of green-house gas point sources, is spatial mis-registration between spectral channels. Different parts of the three spectral bands contribute different information to the retrieval algorithm. The oxygen absorption lines of the O_2 A-band measured in the NIR are used to quantify the ground pressure at the spatial sample, as well as the effective (scattered) photon path in propagation of the measured sunlight thought the atmosphere. The simultaneously measured absorption bands in the SWIR-1 and SWIR-2 are used to quantify the amount of CO_2 molecules along the photon path, and the combination in the three-band retrieval yields the concentration in terms of XCO2. Any spatial mismatch between the NIR and SWIR bands leads to an over- or under-estimation of this concentration, depending on the different columns of air sampled in the NIR and SWIR channels. This error in XCO2 varies primarily with surface height differences and therefore gives rise to a pseudo-noise, which is particularly pronounced over hilly or mountainous terrain. The requirement for this error contribution is therefore driven by surface topography, and translates into the very stringent co-registration requirement of 5% of the spatial sampling distance (SSD). For a square spatial sample of 2km x 2km this corresponds to a spatial mismatch of only 100m between any measured spectral channel, observed from an altitude of 800 km. This required spatial performance is significantly superior to those of comparable space-borne imaging spectrometers (e.g. Sentinel-5 requires 30% of SSD). Flown down to component level, it imposes extremely stringent constraints on image quality, alignment accuracy and stability, which are difficult to achieve by optical and thermo-mechanical design. It is therefore likely that alternative approaches for improving spatial co-registration will be deployed in the greenhouse gas instrument of the CO2M mission.

Possible technologies for improving spatial co-registration involve innovative entrance slit designs based on wave-guides or optical fibers. For example, the fiber-based entrance slits manufactured in the frame of an ESA-initiated pre-development activity [14] are likely to significantly reduce co-registration errors, while at the same time allowing for relaxation of image requirements in terms of keystone and smile distortion. Figure 5 depicts a microscope image of one of these fiber-slit devices with typical dimensions for space-borne imaging spectrometers. The primary purpose of these devices is the reduction of pseudo-noise from non-uniform scenes, which is another significant limitation of retrieval precision. The homogenization functionality and performance has been verified by extensive characterized measurements using an elaborate a test breadboard [20]. As can be seen evident from Figure 5, the entrance slit formed by the stacked array of optical fibers exhibits gaps of typically 30 µm between the individual across-track field-of views, which are due to the cladding around the fiber cores. Since light cannot transmit through the cladding, these gaps will give rise to non-illuminated stripes on the focal plane. On one hand this constitutes a loss of signal and results in a reduction of SNR, which needs to be considered and compensated. On the other hand, these "dark stripes" allow for an unambiguous distinction of the light propagating through each individual fiber, defining the across-track field of view of one spatial sample. The detected electrons from the illuminated detector pixels are co-added in each spectral channel. The near-zero signal between the illuminated areas prevents that photons from neighboring spatial samples is co-added

to the signal, even in presence of large image distortion or detector alignment errors (e.g. rotation). In this way, nearly perfect co-registration can be achieved across all spectral bands, as long as they share the same entrance slit. As an additional advantage, the illumination gaps on the focal plane may be used for in-flight monitoring straylight between the spatial samples across the entire swath width and spectral range.
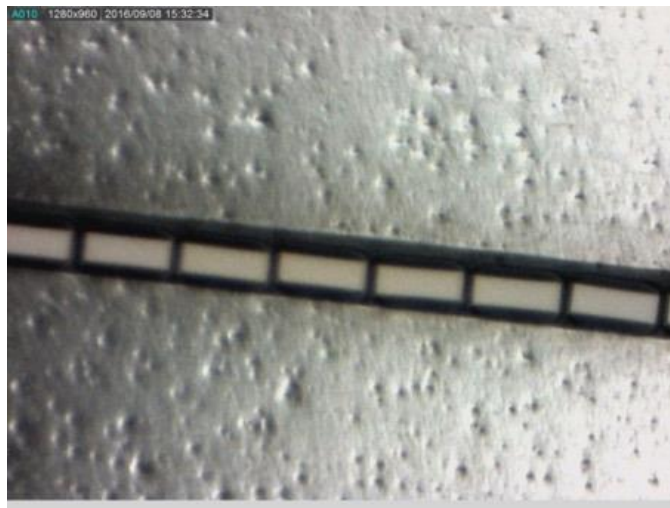

Figure 5: Microscope image of spectrometer entrance slit based stacked optical fibers. The rectangular fiber cores define the slit width in along-track direction (~100 µm), and the spatial sampling distance in across-track direction. The scene heterogeneity is scrambled during propagation through the fiber (~20 mm). The spatial gaps between the fibers is due to the cladding around the cores, and serves to improve spatial co-registration. Courtesy CeramOptec.

5.4 Accuracy (bias) requirements for XCO$_2$ observations

The above sections offered a detailed discussion of requirements, which are deemed to be driving the primary mission goal of CO2M to quantify anthropogenic greenhouse gas emissions from spatially resolved images of CO$_4$ and CH$_4$ concentration. Since anthropogenic carbon fluxes are underlying much larger biogenic ones, the latter also have to accurately measured over larger distances of country- and continental scales. As for the heritage missions like GOSAT and OCO-2, this imposes stringent requirements for low bias observations (< 0.5 ppm). These in turn translate into challenging instrument specifications for straylight performance, polarization sensitivity and detection non-linearity. The approach to constraining these effects is building on heritage from the CarbonSat studies. For the Earth Explorer candidate mission, bias accuracy was specified in terms of a figure-of merit called the Effective Spectral Radiometric Accuracy (ESRA), which is defined as the scalar product of error spectra with so-called gain vectors. Spurious spectral features are simulated for the optical design, e.g. from straylight models, and the deviation from a perfect measurement defines the error spectrum. The gain vectors are computed from a radiative transfer model and the Jacobian matrix composed of the partial derivatives of the TOA radiance w.r.t. the estimated parameters (like CO$_2$ column density). The gain vector approach was explained in detail in a previous conference paper [14]. The gain vectors presented therein have been updated for CO2M instrument, and are plotted in Figure 6. The gains can be interpreted as representing the sensitivity of the retrieved XCO$_2$ to radiometric error. The spectral regions with large gain amplitude contribute proportionally stronger to the total resulting bias in XCO$_2$. Consequently, systematic radiometric biases spectrally correlating with the gains are particularly harmful in the retrieval.
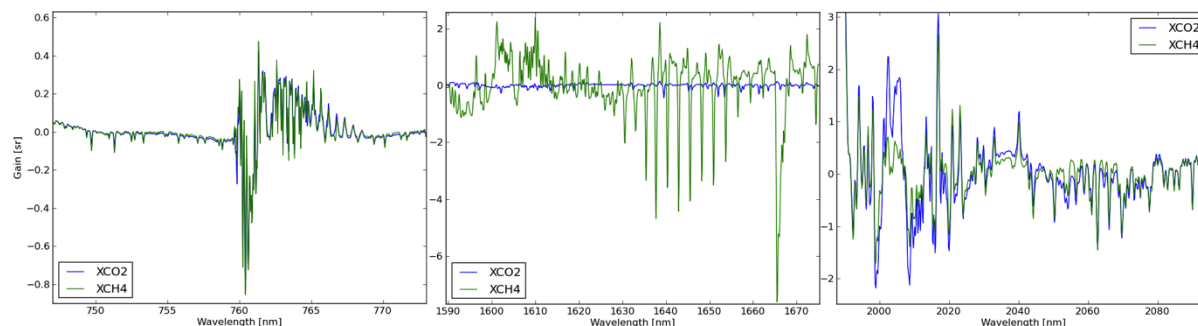
Figure 6: Gain spectra for the retrieval of XCO_2 from spectral radiance measurements at CO2M spectral resolution. These gain spectra or vectors are used to define the requirement constraining spectral features from various instrumental effects, including straylight and polarization sensitivity.

5.5 Requirements for NO_2 observations

In addition, the support studies for the CO2M mission identified the necessity of auxiliary measurements, which significantly enhance the ability to separate anthropogenic CO_2 emissions from natural ones. The wind direction and speed, which are required for flux inversion, can be constrained by co-located observation of nitrogen dioxide (NO_2). Therefore, a spectral interval covering the NO_2 absorption features in the visible (VIS) has been added to the band definition of the CO2M instrument. The measurements in the VIS band are not used in the three-band retrieval for XCO_2, but rather in the subsequent flux-inversion by means of the NO_2 total column product. Therefore there is no stringent co-registration required between the VIS on the one hand, and the NIR and SWIR bands on the other. This allows for implementation of the VIS spectrometer as a separate instrument on the CO2M platform. However, in order to be able to re-sample the NO_2 images onto the spatial grid of the CO_2 observations, very high spatial sampling of the observations is specified at 1 km^2. The spatial resolution, defined as the area over which the SNR and integrated energy requirements are fulfilled, is the same as CO2M at 4 km^2 (2 km x 2km for square samples). This is roughly 6 times higher spatial resolution than the currently highest resolved NO_2 product from the Tropomi instrument of the Sentinel-5P mission [15]. Also the SNR and the spectral resolution requirements are comparable to the heritage missions for atmospheric chemistry. The most important requirements for the VIS band are summarized in Table 3.

Requirement	Value
Spectral band	405nm-490nm
Spectral resolution	0.60 nm
Lref	$1.35 \cdot 10^{13}$ photons/s/cm2/nm/sr
SNR@Lref	500(T)/1000(G)

Table 3.: Main requirements for radiance measurement of the VIS band

5.6 Requirements for Multiple-Angle Polarimeter (MAP) observations

Another set of required auxiliary observations are measurements of spectral radiance and degree of polarization over a broad spectral range and various viewing angles. From measurements of a Multiple-Angle-Polarimeter (MAP) the aerosol distribution above the area under investigation can be inferred, which in turn improves the ability to constrain the

effective photon path in the XCO_2 retrieval. Such measurements have been acquired in the context of instruments targeting aerosol studies, such as POLDER [17] and are proposed for the future 3MI mission [18]. These instruments provide observations of radiance and the Degree of linear polarization (DoLP) for a set of spectral bands and a few tens of viewing angles. This observation strategy with bandwidths of typically > 10 nm in the NIR, VIS and SWIR regions is referred to as MAP-band method.

More recently, a new approach to aerosol observation has been proposed for the PACE mission. The technique, based on the SPEX instrument concept [19], employs a radiometric modulation of an acquired, continuous radiance spectrum, whereby the modulation depth depends on the degree of linear polarization (DOLP). In comparison with the MAP-band method, the modulation technique (MAP-mod) required less viewing angles (less than ten), but higher spectral resolution on the order of 2-4 nm. The required bandwidth of the continuously sampled spectra encompasses the VIS and NIR spectral regions.

Since both techniques, MAP-band and MAP-mod, are regarded as equally suitable approaches to constraining aerosol distribution for enhanced XCO_2 retrieval, two different sets of requirements have been established for CO2M constellation, which are summarized in Table 4 and 5. Due to the distinctiveness of the two measurement techniques, the spectral and radiometric, as well as the geometric requirements (in terms of required viewing angle) are quite different. The two major common features are the spatial sampling distance of the re-sampled Level-1b data (4 km^2) and the polarimetric accuracy and precision (both 0.0025 of DoLP).

Channel	Central Wavelength	Spectral Resolution	DoLP
	(nm)	(nm)	
MAP-1	410	20	Y
MAP-2	443	20	Y
MAP-3	490	20	Y
MAP-4	555	20	Y
MAP-5	670	20	Y
MAP-6 (G)	763	10	N
MAP-7 (G)	765	40	N
MAP-8	865	40	Y

Table 4: Spectral requirements of radiance and polarimetric measurements for the MAP based on the bandpass concept (MAP-band)

Observable	Spectral Range (nm)	Spectral Resolution (nm)
Radiance measurements	385-770	5
DoLP measurements	385-770	15 @ 385 nm 40 @ 755 nm

Table 5: Spectral requirements of radiance and polarimetric measurements for the MAP based on the modulation concept (MAP-mod)

6. SUMMARY AND CONCLUSIONS

We have presented the payload components and most important observational requirements of the CO2M mission. The payload is comprised of a suite of instruments, performing simultaneous, co-located observations. The primary CO_2 instrument measuring in the three spectral bands is complemented auxiliary payloads consisting in a visible spectrometer for NO_2 observation, a multiple-angle polarimeter and a cloud imager. The objective of detecting and quantifying anthropogenic emissions drives the instrument to high single-sounding precision (low random error) of the Level-2 images of XCO_2, Dedicated analysis emphasizes the importance of minimizing random retrieval noise to ensure detectability of emission plumes with faint differential absorption signals. We have presented a method, which translates the required Level-2 retrieval precision into a simple requirement for signal-to-noise ratio of the CO_2 instrument. The requirement derivation establishes a general link between Level-2 and Level-1b observations without assuming particular instrument setups. The need for low bias observations of XCO_2 are comparable to previous and planned missions, imposing low systematic errors of the measurements.

REFERENCES

[1] "Paris Agreement", United Nations Treaty Collection, C.N.92.2016.TREATIES-XXVII.7.d, July 2016

[2] Pinty B., G. Janssens-Maenhout, M. Dowell, H. Zunker, T. Brunhes, P. Ciais, D. Dee, H. Denier van der Gon, H. Dolman, M. Drinkwater, R. Engelen, M. Heiman, K. Holmlund, R. Husband, A. Kentarchos, Y. Meijer, P. Palmer and M. Scholze: An Operational Anthropogenic CO2 Emissions Monitoring & Verification Support capacity - Baseline Requirements, Model Components and Functional Architecture, doi:0.2760/08644, European Commission Joint Research Centre, EUR 28736 EN, 2017

[3] Ciais, P., D. Crisp, H. Denier Van Der Gon, R. Engelen, M. Heimann, G. Janssens-Maenhout, P. Rayner, and M. Scholze, Towards a European Operational Observing System to Monitor Fossil CO2 emissions, Final Report, European Commission, Oct. 2015

[4] Buchwitz, M., R. de Beek, J. P. Burrows, H. Bovensmann, T. Warneke, J. Notholt, J. F. Meirink, A. P. H. Goede, P. Bergamaschi, S. Körner, M. Heimann, and A. Schulz, Atmospheric methane and carbon dioxide from SCIAMACHY satellite data: Initial comparison with chemistry and transport models, Atmos. Chem. Phys., 5, 941-962, 2005

[5] Crisp, D., et al., The Orbiting Carbon Observatory (OCO) mission, Adv. Space Res., 34, 700-709, 2004.

[6] Kuze, A., Suto, H., Nakajima, M., and Hamazaki, T.: Thermal and near infrared sensor for car- bon observation Fourier-transform spectrometer on the Greenhouse Gases Observing Satellite for greenhouse gases monitoring, Applied Optics, 48, 6716–6733, doi:10.1364/AO.48.006716

[7] Crisp, D., Miller, C. E., and DeCola, P. L.: NASA Orbiting Carbon Observatory: measuring the column averaged carbon dioxide mole fraction from space, Journal Of Applied Remote Sensing, 2, 23 508, doi:10.1117/1.2898457, 2008.

[8] Nassar, R., Hill, T. G., McLinden, C. A., Wunch, D., Jones, D. B. A., & Crisp, D. (2017). Quantifying CO2 emissions from individual power plants from space. Geophysical Research Letters, 44, 10,045–10,053. https://doi.org/10.1002/ 2017GL074702

[9] Liu Yi and the TanSat Science Team, "The Pre-launch Status of TanSat Mission," 12th International Workshop on Greenhouse Gas Measurements from Space (IWGGMS-12)," Kyoto University, Kyoto, Japan, June7- 9, 2016, URL: https://www.omc.co.jp/iwggms12/pdf/Session_9/42_Yi_Liu.pdf

[10] Dongxu Yang, Yi Liu, Zhaonan Cai, Xi Chen, Lu Yao, Daren Lu, "First Global Carbon Dioxide Maps Produced from TanSat Measurements," Advances in Atmospheric Sciences, Vol. 35(6), 2018, pp: 621–623, https://doi.org/10.1007/s00376-018-7312-6, URL: https://link.springer.com/content/pdf/10.1007%2Fs00376-018-7312-6.pdf

[11] Pasternak, F., Bernard, P., Georges, L., Pascal, V.,: The MicroCarb instrument, Proceedings Volume 10562, International Conference on Space Optics — ICSO 2016; 105621P (2017) https://doi.org/10.1117/12.2296225

[12] O'Brien, D. M., Polonsky, I. N., Utembe, S. R., and Rayner, P. J.: Potential of a geostationary geoCARB mission to estimate surface emissions of CO2, CH4 and CO in a polluted urban environment: case study Shanghai, Atmos. Meas. Tech., 9, 4633-4654, https://doi.org/10.5194/amt-9-4633-2016, 2016

[13] Sierk, B., Caron, J., Bézy, J.-L., Löscher, A., ; Meijer, Y., Jurado, P., The CarbonSat candidate mission for imaging greenhouse gases from space: concepts and system requirements, Proceedings Volume 10563, International Conference on Space Optics — ICSO 2014; 105633I (2017) https://doi.org/10.1117/12.2304154

[14] Sierk, B., Löscher, A., Caron, J., Bézy, J.-L., Meijer, Y., CarbonSat instrument pre- developments: Towards monitoring carbon dioxide and methane concentrations from space, Proceedings Volume 10562, International Conference on Space Optics — ICSO 2016; 1056260 (2018) https://doi.org/10.1117/12.2322406

[15] Veefkind, P., et al.: Overview of Early Results from TROPOMI on the Copernicus Sentinel 5 Precursor, 20th EGU General Assembly, EGU2018, Proceedings from the conference held 4-13 April, 2018 in Vienna, Austria, p.12216

[16] Wu, L., Hasekamp, O., Hu, H., Landgraf, J., Butz, A., de Brugh, J. a., et al. (2018). Carbon dioxide retrieval from OCO-2 satellite observations using the RemoTeC algorithm and validation with TCCON measurements. *Atmospheric Measurement Techniques, 11*(5), 3111-3130. doi:10.5194/amt-11-3111-2018.

[17] P.-Y. Deschamps, F.-M. Bréon, M. Leroy, A. Podaire, A, Bricaud, J.-C. Buriez, and G. Sèze, "The POLDER mission: Instrument Characteristics and Scientific Objectives," IEEE Transactions On Geoscience and Remote Sensing 32(3), pp. 598-615, May 1994

[18] I. Manolis, S. Grabarnik, J. Caron; J-L. Bézy; M. Loiselet; M. Betto; H. Barré; G. Mason; R. Meynart, "The MetOp second generation 3MI instrument," in Proc. SPIE 8889, Sensors, Systems, and Next- Generation Satellites XVII, October 2013

[19] van Amerongen, A., Rietjens, J., Smit, M., van Loon, D., van Brug, H., van der Meulen, W., Esposito, M., Hasekamp, O.: SPEX: the Dutch roadmap towards aerosol measurement from space, International Conference on Space Optics (ICSO) 2016

[20] Amann, S. Duong-Ederer, Q., Haist, T., Sierk, B., Guldimann. B., Osten, W.: Characterization of fiber-based slit homogenizer devices in the NIR and SWIR, International Conference on Space Optics (ICSO) 2018